HOKKAIDO UNIVERSITY

Title	Condensation coefficient of water in a weak condensation state
Author(s)	Kobayashi, Kazumichi; Watanabe, Shunsuke; Yamano, Daigo et al.
Citation	Fluid Dynamics Research, 40(7-8), 585-596 https://doi.org/10.1016/j.fluiddyn.2007.12.011
Issue Date	2008
Doc URL	https://hdl.handle.net/2115/46997
Rights	Copyright © (2008) IOP Publishing Ltd. This is an author-created, un-copyedited version of an article accepted for publication in Fluid Dynamics Research. IOP Publishing Ltd is not responsible for any errors or omissions in this version of the manuscript or any version derived from it. The definitive publisher-authenticated version is available online at 10.1016/j.fluiddyn.2007.12.011.
Type	journal article
File Information	Kobayash_FDR_2008.pdf

Hokkaido University Collection of Scholarly and Academic Papers : HUSCAP

Condensation Coefficient of Water in a Weak Condensation State

Kazumichi Kobayashi * Shunsuke Watanabe**
Daigo Yamano** Takeru Yano** and Shigeo Fujikawa**

* *Division of Mechanical Engineering, Osaka Prefecture University, 1-1 Gakuen-cho, Naka-ku, Sakai, Osaka 599-8531, Japan*

** *Division of Mechanical and Space Engineering, Hokkaido University, Kita 13 Nishi 8, Sapporo, Hokkaido 060-8628, Japan*

Abstract

The condensation coefficient of water at a vapor-liquid interface is determined by combining shock tube experiments and numerical simulations of the Gaussian-BGK Boltzmann equation. The time evolution in thickness of a liquid film, which is formed on the shock tube endwall behind the shock wave reflected at the endwall, is measured with an optical interferometer consisting of the physical beam and the reference one. The reference beam is utilized to eliminate systematic noises from the physical beam. The growth rate of the film is evaluated from the measured time evolution and it is incorporated into the kinetic boundary condition for the Boltzmann equation. From a numerical simulation using the boundary condition, the condensation coefficient of water is uniquely deduced. The results show that, in a condition of weak condensation near a vapor-liquid equilibrium state, the condensation coefficient of water is almost equal to the evaporation coefficient estimated by molecular dynamics simulations near a vapor-liquid equilibrium state and it decreases as the system becomes a nonequilibrium state. The condensation coefficient of water is nearly identical with that of methanol (Mikami *et al.*, 2006).

Key words: condensation coefficient, water, molecular gas dynamics, shock tube

* Email address: kobakazu@me.osakafu-u.ac.jp

1 Introduction

Evaporation and condensation are fundamental processes of a vapor-liquid interface in various fields of science and technology. To deal with physics of evaporation and condensation, molecular gas dynamics is one of essential tools because evaporation and condensation processes are nonequilibrium phenomena and thus they cannot be dealt with by fluid mechanics based on continuum hypothesis. Until the present, various fruitful results on physics of evaporation and condensation have been obtained by using molecular gas dynamics, e.g., see the books written by Cercignani (2000); Sone (2002, 2006) and references therein.

An unresolved problem lasting for about one century is determination of two unknown parameters, which have values from zero to unity, involved in the kinetic boundary condition at a vapor-liquid interface. One is the evaporation coefficient, which is defined as the ratio of the mass flux of spontaneously evaporating molecules from the interface to the total mass flux going out from it in an equilibrium state. Recently, it has been shown, by molecular dynamics simulations conducted by Ishiyama *et al.* (2004), that the evaporation coefficient depends on only the temperature of the condensed phase. Ishiyama *et al.* (2004) have evaluated accurate values of the evaporation coefficient for argon, water and methanol at various temperatures. The other is the condensation coefficient, which is defined as the ratio of the condensed mass flux of molecules to the flux colliding onto the interface. In an equilibrium state, the evaporation and condensation coefficients are equal from the definitions of these coefficients. Numerous studies have been made to determine the evaporation or condensation coefficient, e.g., see the review paper written by Marek and Straub (2001). However, widely scattered values have given rise to much controversy.

Fujikawa *et al.* (1987) have developed a unique method for determination of the condensation coefficient by combining the measurement of condensation rate of a vapor in a shock tube with a theoretical counterpart based on the Navier-Stokes equations together with the hydrodynamical kinetic boundary condition (Sone and Onishi, 1978). Recently, the present authors (Yano *et al.*, 2003; Fujikawa *et al.*, 2004; Kobayashi *et al.*, 2005) have improved Fujikawa *et al.*'s theoretical counterpart by adopting the polyatomic version of the Gaussian-BGK Boltzmann equation (Andries *et al.*, 2000). The authors have thereby determined successfully the condensation coefficient of methanol in vapor-liquid nonequilibrium states (Mikami *et al.*, 2006). As a result, it has been clarified that the condensation coefficient of methanol near equilibrium states is almost equal to the evaporation coefficient predicted by Ishiyama *et al.*'s molecular dynamics simulations at equilibrium states (Ishiyama *et al.*, 2004) and the condensation coefficient decreases as a vapor-liquid system devi-

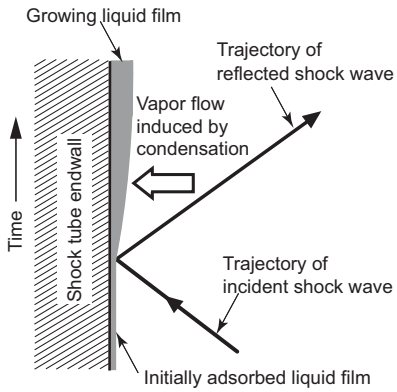

Fig. 1. The growth of the liquid film on the shock tube endwall behind the shock wave reflected at the liquid surface.

ates from an equilibrium one. The present paper aims at determining exactly the condensation coefficient of water in vapor-liquid nonequilibrium states. The reason for using water is that water is one of the most important liquids in various fields and its condensation coefficient has not yet been determined exactly.

2 Methods

2.1 Problem statement

The condensation coefficient can be determined from both the measurement of net condensation rate of a vapor in a vapor-liquid nonequilibrium state and the theoretical counterpart based on the Gaussian-BGK Boltzmann equation. The measurement of condensation rate in an equilibrium state is impossible because the net condensation rate is null in such condition. Therefore, a vapor-liquid system must be shifted from an equilibrium state to a nonequilibrium one in a time scale of molecular mean free time of vapor molecules, and after that the measurement of net condensation rate must be performed within a time scale of the order of microseconds during the process that the nonequilibrium state is changing to a new equilibrium one.

A shock tube is a suitable device to realize a nonequilibrium state at the vapor-liquid interface (Fujikawa *et al.*, 1987; Mikami *et al.*, 2006). Figure 1 shows the propagation process of shock waves in a vapor advancing toward and reflecting from the endwall of a shock tube. Just at the instant when the shock wave is reflected at the endwall on which an adsorbed liquid film with a thickness of a molecular scale exists initially, the pressure, temperature and density of the vapor far from the endwall increase rapidly and these are held at higher values compared with the initial ones. However, the vapor temperature

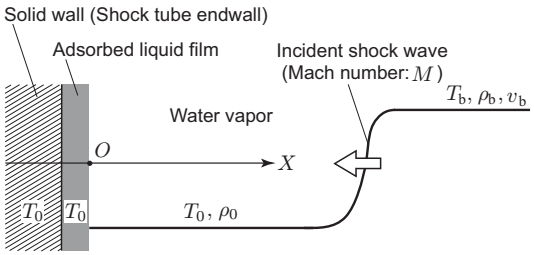

Fig. 2. The schematic diagram of numerical model.

adjacent to the endwall changes little because the endwall made of a thick glass has a large heat capacity compared with that of the vapor, whereas the vapor pressure increases almost to the pressure in the main stream. Thus, the vapor becomes supersaturated at the surface of the adsorbed liquid film, and it begins to condense in the form of a liquid film on the adsorbed film. The liquid film grows with the lapse of time to a macroscopic scale.

2.2 Determination method of condensation coefficient

2.2.1 Numerical analysis

The numerical analysis is conducted for the problem mentioned in *Problem statement*. As shown in Fig. 2, a steady shock wave in a vapor with plane front is formed far from the endwall and propagates toward it. In front of the incident shock wave with Mach number M, the molecular distribution function is a stationary Maxwellian with the temperature T_0 and the density ρ_0. Behind the shock wave, the distribution function is also Maxwellian with T_b, ρ_b and the velocity v_b. These quantities both in front of and behind the shock wave can be connected by Rankine-Hugoniot relations. An adsorbed liquid film is supposed to exist initially on the endwall, as it does actually. After the shock wave is reflected at the endwall, the condensation takes place filmwise on the surface of the initially adsorbed liquid film, and the liquid film grows with the lapse of time. The temperatures of the liquid film and endwall change due to the release of latent heat of condensation. Therefore, we need to solve the Boltzmann equation for the vapor together with the heat conduction equations for the liquid film and endwall. We assume that this phenomenon is a one-dimensional problem. The coordinate X stems from the moving vapor-liquid interface. The Gaussian BGK-Boltzmann equation is adopted as the governing equation for the water vapor and given by

$$\frac{\partial f}{\partial t} + (\xi_x - v_\ell)\frac{\partial f}{\partial X} = \frac{p}{\mu(1-\nu+\theta\nu)}\Big(G(f) - f\Big), \tag{1}$$

where $f(X, t, \boldsymbol{\xi}, \eta)$ is the molecular distribution function, t the time, $\boldsymbol{\xi} = (\xi_x, \xi_y, \xi_z)$ the molecular velocity in which ξ_x, ξ_y, ξ_z are the x-, y-, z-components,

η the internal energy parameter, v_ℓ the velocity of the moving interface, p the vapor pressure, $\mu(T)$ the viscosity coefficient which is a function of the vapor temperature T, and ν and θ are constants. The function $G(f)$ in the right hand side of Eq. (1) is given by

$$G(f) = \rho \hat{f}^G_{\rm tr} \hat{f}^G_{\rm int}, \tag{2}$$

$$\hat{f}^G_{\rm tr} = \frac{1}{\sqrt{\det(2\pi\tau_{ij})}} \exp\Big(-\frac{1}{2}(\xi_i - v_i)\tau^{-1}_{ij}(\xi_j - v_j)\Big), \tag{3}$$

$$\hat{f}^G_{\rm int} = \frac{1}{\Gamma(\frac{n}{2}+1)(RT_{\rm rel})^{n/2}} \exp\Big(-\frac{\eta^{2/n}}{RT_{\rm rel}}\Big), \tag{4}$$

where ρ is the vapor density, $\hat{f}^G_{\rm tr}$ the translational distribution function of polyatomic molecules, $\hat{f}^G_{\rm int}$ the distribution function of internal motions, det the determinant, Γ the gamma function, R the gas constant and n the internal degree of freedom of vapor molecules which is taken to be 3 for water so that the theoretical specific heat ratio ($\gamma = 8/6$) can coincide with the experimental one. The other quantities are defined by

$$\rho = \iint f \mathbf{d}\boldsymbol{\xi} {\rm d}\eta, \quad \rho v_x = \iint \xi_x f \mathbf{d}\boldsymbol{\xi} {\rm d}\eta, \quad \frac{3}{2} RT_{\rm tr} = \frac{1}{\rho}\iint \frac{1}{2}(\xi_i - v_i)^2 f \mathbf{d}\boldsymbol{\xi} {\rm d}\eta,$$
$$\frac{n}{2} RT_{\rm int} = \frac{1}{\rho}\iint \eta^{2/n} f \mathbf{d}\boldsymbol{\xi} {\rm d}\eta, \quad T = \frac{3}{n+3} T_{\rm tr} + \frac{n}{n+3} T_{\rm int}, \quad p = \rho RT,$$
$$T_{\rm rel} = \theta T + (1-\theta) T_{\rm int}, \quad \rho\Theta_{ij} = \iint (\xi_i - v_i)(\xi_j - v_j) f \mathbf{d}\boldsymbol{\xi} {\rm d}\eta,$$
$$\tau_{ij} = (1-\theta)[(1-\nu) RT_{\rm tr}\delta_{ij} + \nu\Theta_{ij}] + \theta RT\delta_{ij},$$

where v_x is the velocity component of x direction, $T_{\rm tr}$ the translational temperature, $T_{\rm int}$ the internal temperature, $T_{\rm rel}$ the relaxation temperature, $\rho\Theta_{ij}$ the stress tensor, τ_{ij} the corrected tensor and δ_{ij} Kronecker's delta. The integration with respect to $\boldsymbol{\xi}$ is carried out over the whole space of $\boldsymbol{\xi}$ unless otherwise stated, and the integration with respect to η is carried out in the domain of $[0, \infty)$.

The Gaussian-BGK Boltzmann equation is solved with the following kinetic boundary condition for molecules going out from the vapor-liquid interface;

$$f^{\rm out} = [\alpha_{\rm e}\rho^* + (1-\alpha_{\rm c})\sigma] \hat{f}^{\rm eq}_{\rm tr} \hat{f}^{\rm eq}_{\rm int}, \quad \text{for} \ \ \xi_x > v_\ell, \tag{5}$$

$$\hat{f}^{\rm eq}_{\rm tr} = \frac{1}{(2\pi RT_\ell)^{3/2}} \exp\Big(-\frac{(\xi_x - v_\ell)^2}{2RT_\ell} - \frac{\xi_y^2 + \xi_z^2}{2RT_\ell}\Big), \tag{6}$$

$$\hat{f}^{\rm eq}_{\rm int} = \frac{1}{\Gamma(\frac{n}{2}+1)(RT_\ell)^{n/2}} \exp\Big(-\frac{\eta^{2/n}}{RT_\ell}\Big), \tag{7}$$

where $\alpha_{\rm e}$ is the evaporation coefficient, $\alpha_{\rm c}$ the condensation coefficient, $\rho^* = p^*/RT_\ell$ the saturated vapor density at the temperature T_ℓ of the liquid film surface, p^* the saturated vapor pressure evaluated from Antoine's formula,

and

$$\sigma = -\sqrt{\frac{2\pi}{RT_\ell}} \iint_{\xi_x < v_\ell} (\xi_x - v_\ell) f^{\mathrm{coll}} \mathbf{d}\boldsymbol{\xi} \mathrm{d}\eta, \tag{8}$$

where f^{coll} is the molecular distribution function incident on the interface.

The condensation coefficient will be determined by the method proposed by Kobayashi *et al.* (2005). The method focuses on the net condensation mass flux at the interface. The flux $\rho_\ell v_\ell$ can be given by the mass conservation equation at the interface;

$$\rho_\ell v_\ell = (\alpha_{\mathrm{c}}\sigma - \alpha_{\mathrm{e}}\rho^*)\sqrt{\frac{RT_\ell}{2\pi}}, \tag{9}$$

where ρ_ℓ is the density of the liquid film. When the vapor-liquid system is in an equilibrium state, $\rho^* = \sigma$ and $\rho_\ell v_\ell$ equal zero and hence $\alpha_{\mathrm{e}} = \alpha_{\mathrm{c}}$. Making use of Eq. (9) allows us to eliminate the evaporation coefficient α_{e} and the condensation coefficient α_{c} from Eq. (5) and leads to

$$f^{\mathrm{out}} = \left(\sigma - \rho_\ell v_\ell \sqrt{\frac{2\pi}{RT_\ell}}\right) \hat{f}^{\mathrm{eq}}_{\mathrm{tr}} \hat{f}^{\mathrm{eq}}_{\mathrm{int}}, \quad \text{for} \quad \xi_x > v_\ell. \tag{10}$$

Therefore, once v_ℓ is experimentally given as a function of time, the Boltzmann equation can be uniquely solved with the distribution function f^{out} given by Eq. (10). In consequence, $\rho_\ell v_\ell$, T_ℓ, ρ^* and σ in Eq. (9) become known, and the unknowns in Eq. (9) are only α_{e} and α_{c}. Note that α_{e} is a function of T_ℓ alone from its definition. Therefore α_{c} can be evaluated from Eq. (9) by using the value of α_{e} which has been estimated by the recent molecular dynamics simulations for water (Ishiyama *et al.*, 2004).

2.2.2 Experimental method

Figure 3 shows the schematic of a horizontal type of shock tube used in the experiment. The length of the low pressure section (test section) is 2830 mm, while the length of the high pressure section is 2600 mm. Two sections are connected coaxially, and a thin aluminum diaphragm is sandwiched between them. The cross section of the shock tube is the circle of 74.3 mm in diameter. The endwall of the test section consists of a quartz glass with the thickness of 15 mm, and the surface is polished at the flatness level of $\lambda/20$ (λ=632.8 nm) to prevent the diffused reflection of a laser beam for optical measurement and to make the laser-shed region of a liquid film on the surface as uniform as possible.

Water vapor is used as the test gas. Experiments are carried out in room temperatures. The shock tube is first evacuated by a vacuum pump, and the

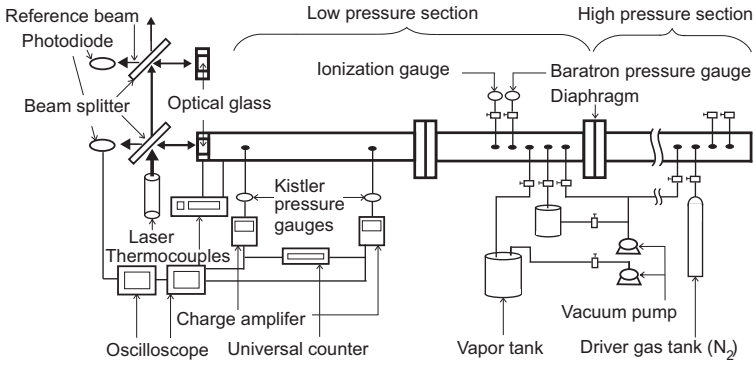

Fig. 3. The schematic diagram of experimental setup.

attained vacuum level of the test section is 1.0×10^{-2} Pa which is measured by an ionization gauge. Then pure water vapor is introduced into the test section from the vapor tank. When a high-pressure driver gas (N_2 gas) is introduced into the high pressure section, the diaphragm is naturally ruptured by a pressure difference between the driver gas and the test vapor. Then a shock wave is generated and propagates toward the endwall in the test section. The Mach number of incident shock wave is estimated from the distance (=1000 mm) between two pressure gauges (type 701A Kistler Instrument AG, Winterthur, Switzerland) and the passage time of the shock wave between them.

The variation in time of a liquid film thickness is obtained by the measurement of light reflectance from the optically transparent film system, because the growing film, together with the glass endwall, forms a kind of interferometer. In the measurement of light reflectance, the following special device is made to eliminate systematic noises from the light reflectance. A light beam from the light source is divided into two beams; one is the physical beam containing information of the liquid film thickness and the other is the reference one which is subtracted from the light reflectance of the physical beam in order to eliminate the noises. The physical and reference beams are detected by two photodiodes, respectively.

3 Results

Figures 4(a) and (b) show both time evolutions of light reflectance; Fig. 4(a) raw data of reflectance of the physical beam (A) and the reference beam (B), Fig. 4(b) datum treated by (A)−(B). In these figures, all data are indicated by voltage. The reflectance (A) shown in Fig. 4(a) is found to be disturbed by a systematic noise which appears before condensation onset and prevents us seriously from evaluating the thickness of the liquid film. The same systematic noise as that in (A) appears in the reflectance (B). Figure 4(b) shows the datum of (A)−(B), and the systematic noise is successfully eliminated.

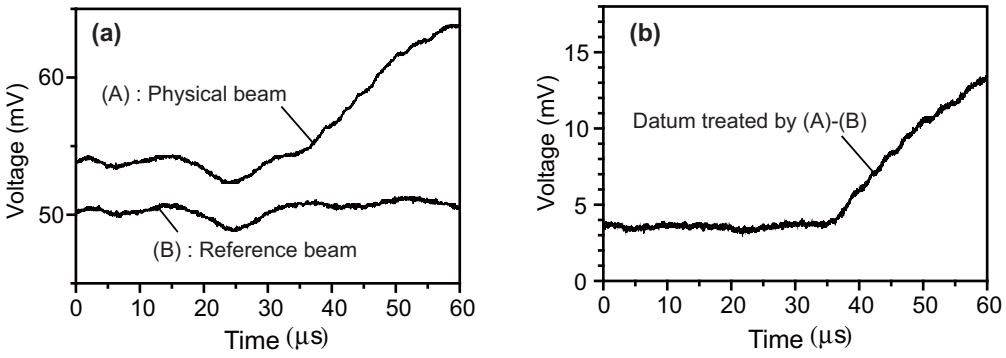

Fig. 4. The measured light reflectance converted into voltage. Initial temperature T_0=290.25 (K), initial pressure p_0=321.3 (Pa) and incident shock Mach number M=1.91: (a) raw data of beams; (b) datum treated by (A)−(B).

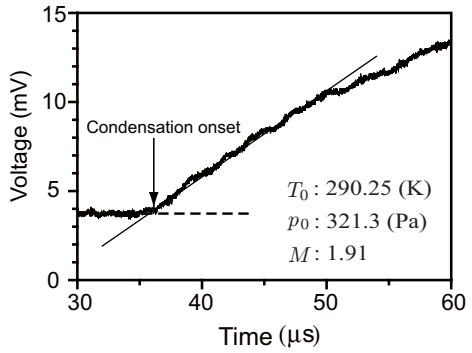

Fig. 5. The determination method of the time of condensation onset for the data of Fig. 4.

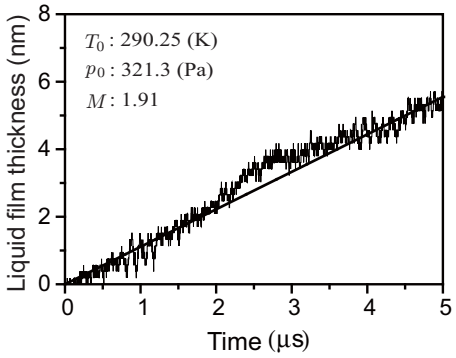

Fig. 6. The liquid film thickness for the datum of Fig 4.

Figure 5 shows the instant of condensation onset and the approximated curve of light reflectance. The dashed line denotes the average value for the time before the condensation onset. Before the onset, the surface of initially adsorbed liquid film can be considered to remain unchanged. By condensation, the light reflectance varies almost in proportion to the time for 5μs. The variation during this time is well approximated by a solid straight line determined by the least square method. The onset time is defined at the intersection point of the solid and dashed lines. Figure 6 shows the variation in time of the liquid film thickness obtained from Fig. 5 with the optical theory (Fujikawa *et al.*, 2004; Mikami *et al.*, 2006). Note that the origin of the time is reset at the condensation onset. The thick solid line is an approximated curve for the converted experimental data. The slope of the curve means the moving velocity of the surface of liquid film v_ℓ. It is found that the curve can be approximated well by a straight line, i.e. v_ℓ is constant for a short time. By using the velocity v_ℓ for the boundary condition given by Eq. (10), the numerical simulation is conducted and the value of the condensation coefficient can be uniquely deduced.

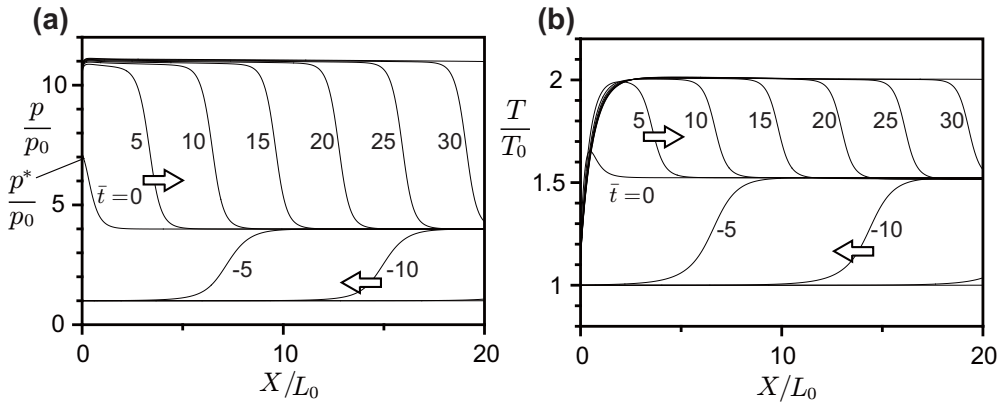

Fig. 7. Propagation processes of the shock waves advancing toward and reflecting from the vapor-liquid endwall; (a) pressure profiles; (b) temperature profiles. The condition is the same as that in Fig. 4, and L_0 denotes the mean free path of vapor molecules in the initial condition.

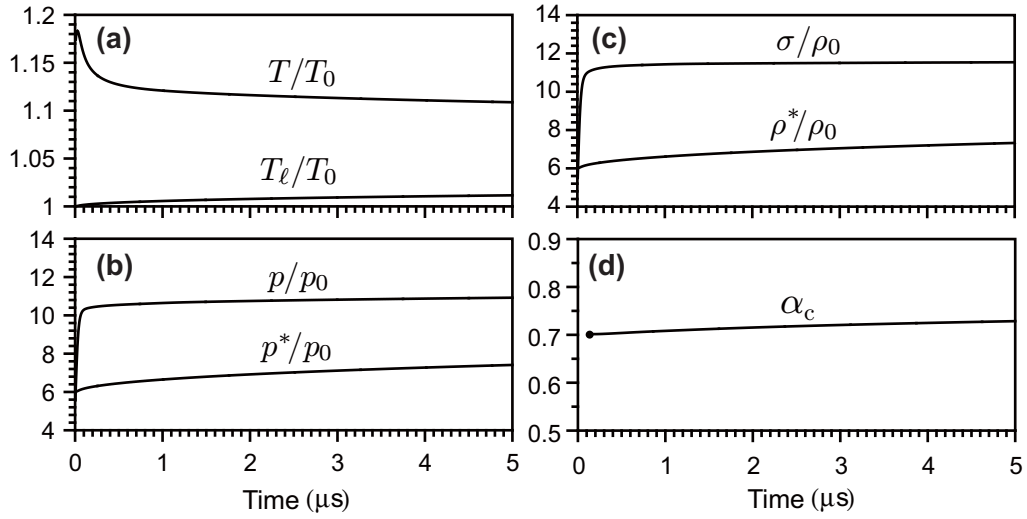

Fig. 8. Variations in time of macroscopic quantities at the vapor-liquid interface and the determined condensation coefficient. The condition is the same as that in Fig. 4.

Figure 7 shows propagation processes of the shock waves advancing toward and reflecting from the vapor-liquid interface: (a) pressure profiles, (b) temperature profiles. The abscissas of (a) and (b) are both the distances from the interface in the vapor, normalized by the mean free path L_0 of vapor molecules in the initial condition. The normalized time $\bar{t} = t/(L_0/\sqrt{2RT_0})$ is indicated for each profile in (a) and (b). The pressure at the interface rises gradually during the incidence and reflection processes of the shock waves and it approaches a constant. On the other hand, the temperature profiles show that the thermal boundary layer including the Knudsen layer, which is the nonequilibrium region of vapor near the interface, is formed behind the reflected shock wave.

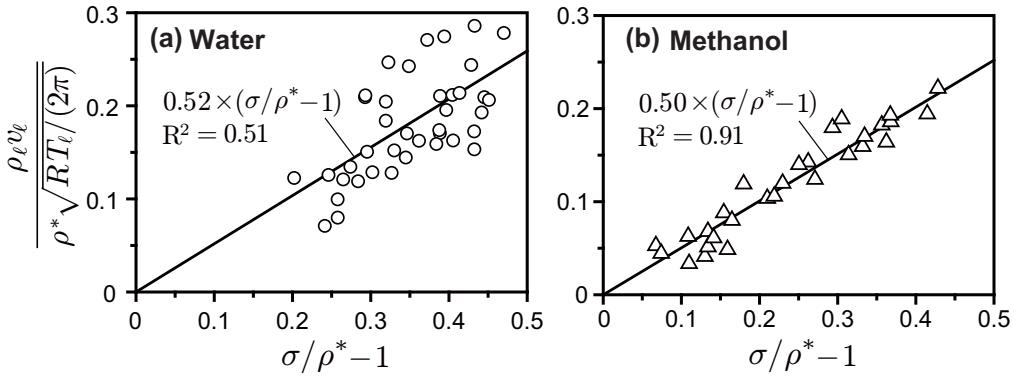

Fig. 9. Mass fluxes at vapor-liquid interfaces versus $\sigma/\rho^* - 1$: (a) water, (b) methanol. The ratio σ/ρ^* is the collision mass flux $\sigma\sqrt{RT_\ell/2\pi}$ onto the interface to the mass flux $\rho^*\sqrt{RT_\ell/2\pi}$ at an equilibrium state.

Figure 8 shows variations in time of macroscopic quantities at the vapor-liquid interface. After the onset time, the vapor temperature T, the pressure p, and σ set in an almost steady state immediately. Then, from Fig. 8(a), one can see that the variation in the liquid film temperature T_ℓ is less than 1%. Therefore, those of the saturated vapor pressure p^* and the saturated vapor density ρ^* are less than 10%. As a result, from Eq. (9), the condensation coefficient α_c may be regarded as a constant value for 5μs after the condensation onset (see Fig. 8(d) and $\alpha_e = 0.86$ in this study).

Figure 9 shows mass fluxes at vapor-liquid interfaces versus $\sigma/\rho^* - 1$ for water (Fig. 9(a)) and methanol (Fig. 9(b)). The results of methanol have been obtained from our previous study (Mikami *et al.*, 2006). Theses results are obtained from 40 experiments for water at the time $t = 2.5\mu$s after the condensation onset and 30 experiments for methanol at $T_\ell = 290$–300 K. The σ/ρ^* of the abscissa denotes the ratio of the collision mass flux $\sigma\sqrt{RT_\ell/2\pi}$ onto the interface to the mass flux $\rho^*\sqrt{RT_\ell/2\pi}$ at equilibrium states. The ordinate is the ratio of the net condensed mass flux $\rho_\ell v_\ell$ to the mass flux $\rho^*\sqrt{RT_\ell/2\pi}$. The vapor-liquid system is in an equilibrium state in the case where σ/ρ^* is unity; hence $\rho_\ell v_\ell = 0$. As the system becomes far from the equilibrium one, the condensation takes place more strongly. The fluctuations in the water case are larger than those in the methanol case because of the small condensation rate of water in the experiments. The thick solid lines are obtained from the least square method for the experimental results. From the figures, we assume that the net mass fluxes are in proportion to $\sigma/\rho^* - 1$, and the relations are given by

$$\frac{\rho_\ell v_\ell}{\rho^*\sqrt{RT_\ell/2\pi}} = A\left(\frac{\sigma}{\rho^*} - 1\right), \tag{11}$$

where $A = 0.52$ for water and $A = 0.50$ for methanol. From the results, we

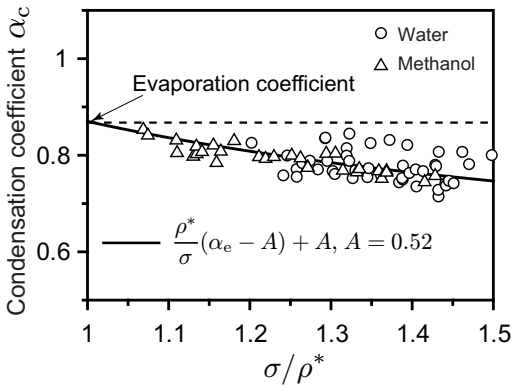

Fig. 10. Condensation coefficients versus σ/ρ^* for water and methanol.

can see that there are similar relations of net condensed mass fluxes at the vapor-liquid interfaces for water and methanol.

Figure 10 shows the relationship between the condensation coefficient and σ/ρ^*. Open circles denote the condensation coefficient of water and open triangles those of methanol. These values are obtained from Eq. (9) by using the evaporation coefficient $\alpha_e = 0.86$ for both water and methanol (Ishiyama *et al.*, 2004). We can see that the condensation coefficient of water changes from 0.84 to 0.71, and that of methanol changes from 0.85 to 0.75, respectively. The condensation coefficients seem to be almost identical values for water and methanol, and these are close to the evaporation coefficient ($\alpha_e = 0.86$) near equilibrium states. From Eqs. (9) and (11), the following equation for the condensation coefficients holds for water and methanol;

$$\alpha_c = \frac{\rho^*}{\sigma}(\alpha_e - A) + A. \tag{12}$$

Equation (12) is shown in Fig. 10 as the solid line, and the condensation coefficients agree with Eq. (12). Consequently, we can estimate the condensation coefficients of water and methanol by using Eq. (12) in weak condensation states at room temperatures.

4 Conclusions

The condensation coefficient of water, which is included in the kinetic boundary condition at a vapor-liquid interface, has been determined by shock tube experiments and numerical simulations of molecular gas dynamics in weak condensation states. The results have shown that the values of condensation coefficient of water are from 0.84 to 0.71 in the range of $\sigma/\rho^* = 1.20$–1.49. From these results, the empirical equations for the condensation coefficients of water and methanol have been obtained in relation to mass fluxes at the interfaces.

Acknowledgments

This work was supported by the Grant in Aid for Scientific Research of the Japan Society for the Promotion of Science from 2005 to 2007(Grant No.17360074: Shigeo Fujikawa) and also the Research Fellowship of the Japan Society for the Promotion of Science for Young Scientists(Kazumichi Kobayashi).

References

Andries, P., Le, Tallec, P., Perlat, J.-P. and Perthame, B. 2000. The Gaussian-BGK model of Boltzmann equation with small Prandtl number, Eur. J. Mech. B-Fluids **19**, 813–830.

Cercignani, C. 2000. Rarefied gas dynamics: from basic concepts to actual calculations. Cambridge University Press.

Fujikawa, S., Okuda, M., Akamatsu, T. and Goto, T. 1987. Non-equilibrium vapour condensation on a shock-tube endwall behind a reflected shock wave, J. Fluid Mech. **183**, 293–324.

Fujikawa, S., Yano, T., Kobayashi, K., Iwanami, K. and Ichijo, M. 2004. Molecular gas dynamics applied to phase change processes at a vapor-liquid interface: shock-tube experiment and MGD computation for methanol, Exp. Fluids **37**, 80–86.

Ishiyama, T., Yano, T. and Fujikawa, S. 2004. Molecular dynamics study of kinetic boundary condition at an interface between polyatomic vapor and its condensed phase, Phys. Fluids **16**, 4713–4726.

Kobayashi, K., Fujikawa, S. and Yano, T. 2005. A new approach for determination of condensation coefficient of methanol by combining molecular gas dynamics study and shock tube experiment, Proc. 6th World Conference on Experimental Heat Transfer, Fluid Mechanics and Thermodynamics, 7-b-7.

Marek, R. and Straub, J. 2001. Analysis of the evaporation coefficient and the condensation coefficient of water, Int. J. Heat and Mass Transf. **44**, 39–53.

Mikami, S., Kobayashi, K., Ota, T., Fujikawa, S., Yano, T. and Ichijo, M. 2006. Molecular gas dynamics approaches to interfacial phenomena accompanied with condensation, Exp. Therm. and Fluid Sci. **30**, 795–800.

Sone, Y. and Onishi, Y. 1978. Kinetic theory of evaporation and condensation: Hydrodynamic equation and slip boundary condition, J. Phys. Soc. Jpn. **44**, 1981–1994.

Sone, Y. 2002. Kinetic theory and fluid dynamics. Birkhäuser.

Sone, Y. 2006. Molecular gas dynamics: theory, techniques, and applications. Birkhäuser.

Yano, T., Kobayashi, K. and Fujikawa, S. 2003. Numerical study of condensation of a polyatomic vapor by a shock wave based on the kinetic theory of gases, Proc. JSME-ASME Fluids Engineering Division Summer Meeting, FEDSM 2003–45022.